INTERNATIONAL JOURNAL FOR NUMERICAL METHODS IN FLUIDS, VOL. 5, 529–543 (1985)

ANALYTIC TEST CASES FOR THREE-DIMENSIONAL HYDRODYNAMIC MODELS

DANIEL R. LYNCH

Thayer School of Engineering, Dartmouth College, Hanover, New Hampshire 03755, U.S.A.

AND

CHARLES B. OFFICER

Department of Earth Sciences, Dartmouth College, Hanover, New Hampshire 03755, U.S.A

SUMMARY

Exact periodic solutions are generated for the 3-D hydrodynamic equations in linearized form. A linear slip condition is enforced at the bottom, based on the velocity at the bottom. It is shown that the bottom stress can be equivalently expressed in terms of the vertically averaged velocity, and expressions for this bottom stress coefficient are derived in terms of the primary parameters of the problem. As a result, the three-dimensional structure may be assembled from conventional solutions to (a) the 1-D vertical diffusion equation; and (b) the 2-D vertically averaged shallow water equations. In the latter, the bottom stress effects are shown to be complex and frequency-dependent, and an additional rotational term is required for their representation.

KEY WORDS Shallow Water Equations Analytic Solutions Three-dimensional

INTRODUCTION AND GOVERNING EQUATIONS

In this paper we develop linearized analytic solutions for periodic, three-dimensional motion in 'shallow' water, i.e. where the wavelength far exceeds the depth. The solutions incorporate the effects of inertia, vertical shear, gravity and rotation, and as such are intrinsically interesting as first-order approximations to the full non-linear motions. Our main purpose, however, is to provide a foundation for the testing of numerical models which will ultimately be used in realistic situations beyond the reach of analysis. In this context the analytic solutions constitute a spectrum of test cases in which the relative strengths of individual physical effects can be precisely controlled, and model performance quantitatively evaluated.

The governing equations of mass and momentum conservation are given in linearized form by Davies.[1] Here we address the periodic form of these, assuming space–time variations of the form $f(\mathbf{x}, t) = \mathrm{Re}(F(\mathbf{x})e^{j\omega t})$:

$$j\omega\zeta + \nabla\cdot(H\bar{\mathbf{V}}) = 0, \tag{1}$$

$$j\omega\mathbf{V} + \mathbf{f}\times\mathbf{V} - \frac{\partial}{\partial z}\left(N\frac{\partial\mathbf{V}}{\partial z}\right) = -g\nabla\zeta, \tag{2}$$

0271–2091/85/060529–15$01.50

Received 30 August 1984
Revised 24 December 1984

where

$\zeta(x, y)$ is the complex amplitude of the free surface elevation
$\mathbf{V}(x, y, z)$ is the complex amplitude of the horizontal velocity
$\bar{\mathbf{V}}(x, y)$ is the vertical average of $\mathbf{V}$
ω is the frequency
j is the imaginary unit, $\sqrt{-1}$
$H(x, y)$ is the bathymetric depth (from undisturbed sea level to bottom)
$\mathbf{f}$ is the Coriolis parameter, directed vertically
$N(x, y, z)$ is the vertical eddy viscosity
g is gravity
(x, y) are the horizontal co-ordinates
z is the vertical co-ordinate, positive upward.

We shall enforce boundary conditions on stress at the free surface and at the bottom:

$$N\frac{\partial \mathbf{V}}{\partial z} = 0, \qquad \text{at } z = 0 \qquad \text{(surface)}, \tag{3}$$

$$N\frac{\partial \mathbf{V}}{\partial z} = k\mathbf{V}, \quad \text{at } z = -H \ \text{(bottom)}, \tag{4}$$

where k is a real linear slip coefficient. In the horizontal, boundary conditions on ζ (pressure) or $\bar{\mathbf{V}}\cdot\mathbf{n}$ will be enforced.

The vertical average* of equation (2) is

$$j\omega\bar{\mathbf{V}} + \mathbf{f}\times\bar{\mathbf{V}} + \frac{N}{H}\frac{\partial \mathbf{V}}{\partial z}\bigg|_{-H} = -g\nabla\zeta, \tag{5}$$

where boundary condition (3) has been incorporated. In the special case where the bottom stress can be related to the average velocity

$$N\frac{\partial \mathbf{V}}{\partial z}\bigg|_{-H} = \tau H\bar{\mathbf{V}}; \tag{6}$$

then $\bar{\mathbf{V}}$ may be eliminated between (1) and (5) to obtain a Helmholtz-type equation for ζ:

$$j\omega\zeta - \nabla\cdot\left[\frac{gH}{(j\omega+\tau)^2 + f^2}((j\omega+\tau)\nabla\zeta - \mathbf{f}\times\nabla\zeta)\right] = 0. \tag{7}$$

The standard procedure in this vertically homogeneous case is then to solve (7) for ζ, after which $\bar{\mathbf{V}}$ may be obtained from (5) and (6). A reasonable suite of such solutions is available for vertically homogeneous model testing.[2–5]

In the present more realistic context, the bottom stress is related as in (4) to the bottom velocity, which may be considerably out of phase with $\bar{\mathbf{V}}$. Several partial solutions are available in which (2) is solved, with boundary conditions (3) and (4), on the premise that the barotropic forcing term $g\nabla\zeta$ is known either *a priori* or from a numerical solution.[6–12] Most of these include the effect of wind stress at the free surface in addition. However full analytic solutions to the equation set (1)–(4) appear to be unavailable.

In the present work we provide exact solutions to equations (1)–(4). A key finding is that the bottom stress may still be expressed in the form (6), i.e. in terms of $\bar{\mathbf{V}}$. However the coefficient τ must

* Throughout we use the overbar to indicate a vertically averaged quantity.

now be complex, indicating a phase shift between bottom stress and $\bar{\mathbf{V}}$. The essential relation between the derived quantity τ and the primary parameters ω, H, N and k is developed and explored. This in turn enables one to invoke existing analytic solutions to (7) for ζ, following which $\mathbf{V}$ may be obtained from (2).

We proceed as follows. First, we solve the general case without rotation and demonstrate the synthesis of the horizontal and vertical structure; this is the foundation of the later analyses. The special case $\partial N/\partial z = 0$, a very simple yet revealing test case, is then examined for illustrative purposes. Finally, we solve the equations with rotation and demonstrate an additional Coriolis-like term in the vertically averaged equations, due to bottom stress.

VERTICAL STRUCTURE AND BOTTOM STRESS WITHOUT ROTATION

The momentum equation in the absence of rotation is

$$\mathbf{V} - \frac{\partial}{\partial Z}\left(\frac{N}{j\omega H^2}\frac{\partial \mathbf{V}}{\partial Z}\right) = \mathbf{V}_0, \tag{8}$$

with boundary conditions

$$\frac{\partial \mathbf{V}}{\partial Z} = 0, \qquad \text{at } Z = 0, \tag{9a}$$

$$K\mathbf{V} - \frac{\partial \mathbf{V}}{\partial Z} = 0, \quad \text{at } Z = -1, \tag{9b}$$

where

$Z = z/H$ is the normalized depth

$K = kH/N|_{-1}$ is the dimensionless slip coefficient

$\mathbf{V}_0 = -g\nabla\zeta/j\omega$ is the depth-invariant, high-frequency limit for $\mathbf{V}$.

Without knowing the gravity term $\mathbf{V}_0(x, y)$, we may nevertheless proceed to solve (8) for the vertical structure at any given point (x, y). A particular solution to (8) is $\mathbf{V} = \mathbf{V}_0$, so the general solution is

$$\mathbf{V} = \mathbf{V}_0 + \mathbf{C}_1\mu_1(Z) + \mathbf{C}_2\mu_2(Z), \tag{10}$$

where the scalar functions μ_1, μ_2 satisfy the homogeneous form of (8). The vectors $\mathbf{C}_1, \mathbf{C}_2$ are independent of Z and are determined by application of (9):

$$\begin{bmatrix} \dot{\mu}_1(0) & \dot{\mu}_2(0) \\ \left.\left(\mu_1 - \frac{1}{K}\dot{\mu}_1\right)\right|_{-1} & \left.\left(\mu_2 - \frac{1}{K}\dot{\mu}_2\right)\right|_{-1} \end{bmatrix} \begin{Bmatrix} \mathbf{C}_1 \\ \mathbf{C}_2 \end{Bmatrix} = \begin{Bmatrix} 0 \\ -\mathbf{V}_0 \end{Bmatrix}, \tag{11}$$

where the overdot indicates $\mathrm{d}/\mathrm{d}Z$. The full solution is therefore

$$\mathbf{V}(x, y, z) = \mathbf{V}_0(x, y)\left[1 + \frac{\dot{\mu}_2(0)\mu_1(Z) - \dot{\mu}_1(0)\mu_2(Z)}{B}\right], \tag{12}$$

where B is the determinant of the matrix in (11).

The vertical average of (12) provides $\bar{\mathbf{V}}$:

$$\bar{\mathbf{V}} = \mathbf{V}_0\left[1 + \frac{\dot{\mu}_2(0)\bar{\mu}_1 - \dot{\mu}_1(0)\bar{\mu}_2}{B}\right]. \tag{13}$$

Additionally, we may relate $\bar{\mu}_i$ to their derivatives by vertically averaging the homogeneous form of (8):

$$\bar{\mu}_i = \frac{N}{j\omega H^2} \dot{\mu}_i \Big|_{-1}^{0}, \qquad i = 1, 2. \tag{14}$$

To make the essential linkage to the vertically averaged equations, the bottom stress is first computed from (12):

$$\frac{N}{H} \frac{\partial \mathbf{V}}{\partial Z}\Big|_{-1} = \frac{\mathbf{V}_0}{B} \left[\dot{\mu}_2(0) \left(\frac{N}{H} \dot{\mu}_1 \right)_{-1} - \dot{\mu}_1(0) \left(\frac{N}{H} \dot{\mu}_2 \right)_{-1} \right], \tag{15}$$

or, equivalently, by exploiting (14),

$$\frac{N}{H} \frac{\partial \mathbf{V}}{\partial Z}\Big|_{-1} = -\frac{j\omega H}{B} \mathbf{V}_0 [\dot{\mu}_2(0)\bar{\mu}_1 - \dot{\mu}_1(0)\bar{\mu}_2]. \tag{16}$$

Finally, the complex bottom stress coefficient, defined on the premise that $(N/H)(\partial \mathbf{V}/\partial Z)/|_{-1}$ may be expressed in the form $\tau H \bar{\mathbf{V}}$, is obtained from (16) and (13):

$$\tau = \frac{-j\omega[\dot{\mu}_2(0)\bar{\mu}_1 - \dot{\mu}_1(0)\bar{\mu}_2]}{[B + \dot{\mu}_2(0)\bar{\mu}_1 - \dot{\mu}_1(0)\bar{\mu}_2]}. \tag{17}$$

Results (12), (13) and (17) may be compactly summarized as

$$\mathbf{V}(x, y, z) = \mathbf{V}_0(x, y) \left[1 - \frac{A(Z)}{B} \right], \tag{18}$$

$$\bar{\mathbf{V}}(x, y) = \mathbf{V}_0(x, y) \left[1 - \frac{\bar{A}}{B} \right], \tag{19}$$

$$\tau(x, y) = \frac{j\omega \bar{A}}{B - \bar{A}}, \tag{20}$$

with

$$A \equiv \det \begin{bmatrix} \dot{\mu}_1(0) & \dot{\mu}_2(0) \\ \mu_1(Z) & \mu_2(Z) \end{bmatrix}, \tag{21}$$

$$B \equiv \det \begin{bmatrix} \dot{\mu}_1(0) & \dot{\mu}_2(0) \\ \left(\mu_1 - \frac{\dot{\mu}_1}{K} \right)_{-1} & \left(\mu_2 - \frac{\dot{\mu}_2}{K} \right)_{-1} \end{bmatrix}. \tag{22}$$

The identity (14) may be used to evaluate $\bar{A}$ without actually averaging the μ_i. A brief collection of homogeneous solutions, for different viscosity structures, appears in Table I.

Observe that the quantities A, $\bar{A}$ and B are implicit functions of (x, y) unless the dimensionless viscosity $N/\omega H^2$ depends on Z alone—otherwise, the homogeneous solutions $\mu(Z)$ will be different at different horizontal locations. Further, B will depend on (x, y) unless in addition the dimensionless slip coefficient $K = (kH/N)|_{-1}$ is constant. For a given physical situation in which $N(x, y, z)$, $H(x, y)$ and $k(x, y)$ are specified, we note that τ will depend on position and frequency, the latter dependence being especially important for motions comprising multiple frequencies.

Finally, note that $\mathbf{V}$ will generally exhibit a phase difference through the vertical. Thus, the actual velocity profile at a point in time, $\mathrm{Re}(\mathbf{V}e^{j\omega t})$, can exhibit a spiral structure when rotation is absent, provided the lateral boundary conditions cause the current to veer over time.

Table I. Solutions to $\left\{\mu-\frac{\mathrm{d}}{\mathrm{d}Z}\left(\frac{N}{j\omega H^2}\frac{\mathrm{d}\mu}{\mathrm{d}Z}\right)=0\right\}$; $Z=\frac{z}{H}$

$N(Z)$	$\mu(Z)$	Notes
$N=N_0$	$\exp\left[\pm Z\sqrt{\left(\frac{j\omega H^2}{N_0}\right)}\right]$	
$N=N_0(Z-Z_0)^2$	$(Z-Z_0)^r$	$r=-\frac{1}{2}\pm\sqrt{\left(\frac{1}{4}+\frac{j\omega H^2}{N_0}\right)}$
$N=N_0(Z-Z_0)^m$ $m\neq 2$ (Reference 11)	$(Z-Z_0)^{(1-m)/2}J_{\pm p}(\alpha)$ $\alpha=\left(\frac{(Z-Z_0)^{(2-m)/2}\sqrt{\left(\frac{-j\omega H^2}{N_0}\right)}}{1-(m/2)}\right)$	J_p = Bessel function of first kind, order p $p=(1-m)/(2-m)$
$N=N_0e^{aZ}$ (Reference 7)	$\xi J_1(\xi\sqrt{(-j)})$; $\xi Y_1(\xi\sqrt{(-j)})$	J_1, Y_1 = Bessel functions of first and second kinds, order 1 $\xi=\frac{2}{a}\sqrt{\left(\frac{\omega H^2}{N_0}\right)}e^{-aZ/2}$
$N=N_0[1+a(Z-Z_0)^2]$	$\sum_{n=0}^{\infty}C_n(Z-Z_0)^n$ $C_{n+2}=C_n\left[\frac{(j\omega H^2/N_0)-a(n+1)(n)}{(n+2)(n+1)}\right]$	C_0, C_1 arbitrary Convergence for $\lvert a(Z-Z_0)^2\rvert<1$

SYNTHESIS OF VERTICAL AND HORIZONTAL STRUCTURE

With the relations (18)–(22), a complete three-dimensional solution may be assembled in three steps:

(1) Evaluate $\tau(x, y)$ for a given frequency component and viscosity structure, via equations (20)–(22).
(2) Use this result to obtain ζ via existing solutions to (7).
(3) Differentiate ζ to obtain $\mathbf{V}_0=-g\nabla\zeta/j\omega$, and use this in (18) to obtain $\mathbf{V}$.

As an example, consider a simple problem of tidal oscillations near a circular island (Figure 1). There is no rotation, and a tide of varying amplitude and uniform phase is specified at $r=r_2$. Bathymetry increases with radius: $H=H_0r^2$. Viscosity is constant through the depth, which leads to the simple homogeneous solutions

$$\mu_{1,2}=\exp\left[\pm Z\sqrt{\left(\frac{j\omega H^2}{N}\right)}\right], \tag{23}$$

and τ is readily evaluated (see equation (33) below). With an eye toward expediency, we keep τ constant, i.e. N/H^2 and kH/N are constants. The horizontal solution to (7) is then obtained from Reference 2:

$$\zeta=(ar^{S_1}+br^{S_2})\cos\theta, \tag{24}$$

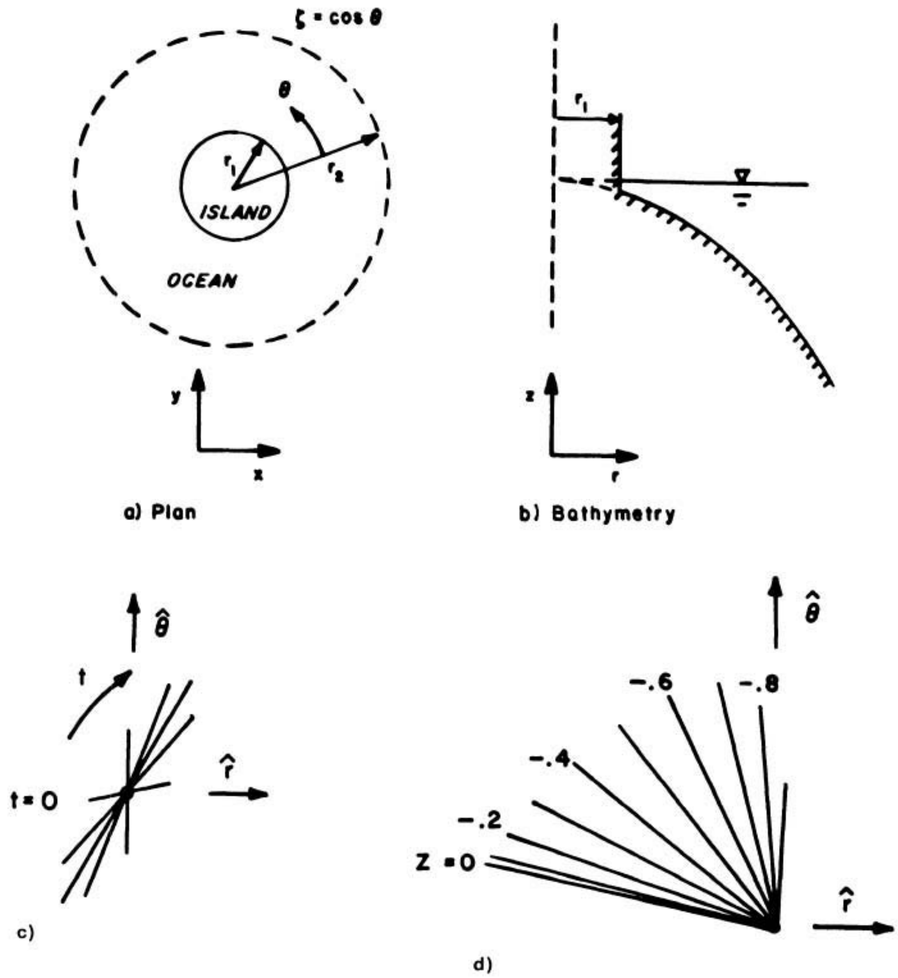

Figure 1. (a, b). Geometry of island example; (c) $\mathbf{V}_0$ at equally spaced time intervals; (d) vertical variations in $\mathbf{V}$ at $t = 0$

where

$$S_1, S_2 = -1 \pm \sqrt{\left[2 - \frac{(\omega^2 - j\omega\tau)}{gH_0}\right]}, \tag{25}$$

$$a = \frac{S_2 r_1^{S_2}}{[S_2 r_2^{S_1} r_1^{S_2} - S_1 r_1^{S_1} r_2^{S_2}]}, \tag{26}$$

$$b = \frac{-S_1 r_1^{S_1}}{[S_2 r_2^{S_1} r_1^{S_2} - S_1 r_1^{S_1} r_2^{S_2}]}. \tag{27}$$

Differentiation of (24) then yields

$$\mathbf{V}_0 = \frac{-g}{j\omega r}[\hat{\mathbf{r}}(S_1 a r^{S_1} + S_2 b r^{S_2})\cos\theta - \hat{\boldsymbol{\theta}}(a r^{S_1} + b r^{S_2})\sin\theta], \tag{28}$$

from which $\mathbf{V}$ may be easily evaluated via (18).

Figures 1(c) and 1(d) display a sample of results for the following parameters: $r_1 = 100\,\text{km}$; $r_2 = 250\,\text{km}$; $\omega = 1{\cdot}4 \times 10^{-4}\,\text{s}^{-1}$; $\omega H^2/N = 10$; $k = \infty$ (no slip); and $H_0 = 10^{-9}\,\text{m}^{-1}$. Figure 1(c) is a vector plot of $\mathbf{V}_0$ at $r = 200\,\text{km}$, $\theta = \pi/4$, at equally spaced time intervals through one period. In Figure 1(d) we plot $\mathbf{V}$ versus normalized depth at $t = 0$ for the same (r, θ) point. At this point in time, the direction of $\mathbf{V}_0$ is changing most rapidly, and the phase lead near the bottom produces substantial veering with depth.

CASE STUDY: CONSTANT VISCOSITY

The obvious point of departure in model testing is the constant viscosity case, and we therefore examine this case in detail. The homogeneous solutions μ_i are exponentials as in (23), and may be expressed in terms of either the dimensionless frequency W or the well-known skin depth δ:

$$\mu_i = \exp[\pm Z\sqrt{(jW)}] = \left[\exp\left(\pm\frac{z}{\delta}\right)\right]\left[\exp\left(\pm\frac{jz}{\delta}\right)\right], \tag{29}$$

where

$W = \dfrac{\omega H^2}{N}$ is the dimensionless frequency

$\delta = \sqrt{\left(\dfrac{2N}{\omega}\right)}$ is the skin depth.

The bottom boundary layer, wherein viscous effects are important, is roughly 4δ in thickness; above this inertia dominates and $\partial\mathbf{V}/\partial z \simeq 0$. The dimensionless frequency is also a measure of depth relative to δ:

$$W = 2\left(\frac{H}{\delta}\right)^2. \tag{30}$$

Thus when $W \gg 1$ the bulk of the flow is independent of depth.

The vertical structure is obtained by straightforward evaluation of (18)–(22):

$$\mathbf{V} = \mathbf{V}_0\left[1 - \frac{\cosh \lambda Z}{(\cosh \lambda)\left(1 + \dfrac{\lambda}{K}\tanh \lambda\right)}\right], \tag{31}$$

$$\bar{\mathbf{V}} = \mathbf{V}_0\left[1 - \frac{\tanh \lambda}{\lambda\left(1 + \dfrac{\lambda}{K}\tanh \lambda\right)}\right], \tag{32}$$

$$\tau = \frac{\tau_0}{3}\left[\frac{\lambda^2 \tanh \lambda}{\lambda + \left(\dfrac{\lambda^2}{K} - 1\right)\tanh \lambda}\right], \tag{33}$$

where

$\lambda = \sqrt{(jW)}$

$\tau_0 = \dfrac{3N}{H^2}$ is the low-frequency, no-slip limit of τ.

In the low-frequency limit, $\tanh\lambda \to \lambda - \lambda^3/3$ and the quasi-static solution is

$$\tau = \frac{\tau_0}{1+\dfrac{3}{K}}, \tag{34}$$

$$\bar{\mathbf{V}} = \mathbf{V}_0\left[\frac{jW}{3}\left(1+\frac{3}{K}\right)\right] = -g\nabla\zeta/\tau, \tag{35}$$

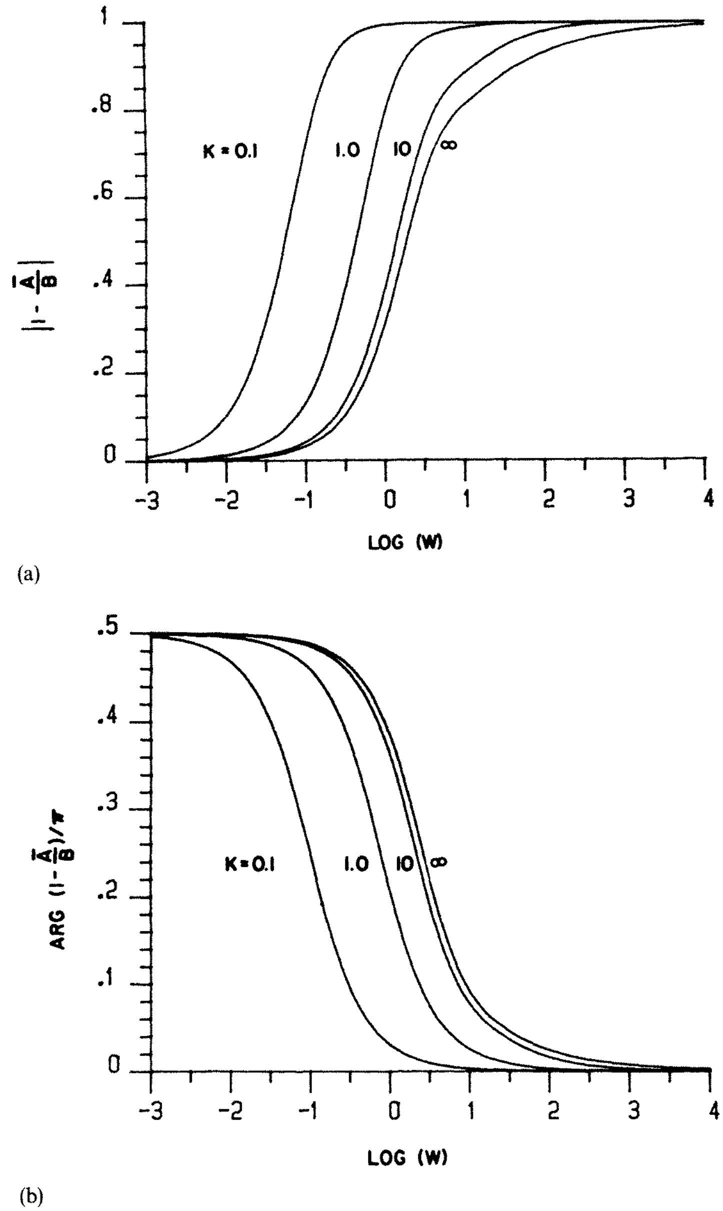

Figure 2. Magnitude (a) and phase (b) of $\bar{\mathbf{V}}$ relative to the high-frequency limit $\mathbf{V}_0$ for constant viscosity

with **V** quadratic in Z. τ is strictly real, as expected. At high frequencies, $\tanh \lambda$ approaches unity and we reach the high-frequency asymptote

$$\tau = \frac{\tau_0 K}{3} = \frac{k}{H}, \tag{36}$$

with $\mathbf{V} = \bar{\mathbf{V}} = \mathbf{V}_0$. Again τ is strictly real. In addition there is the possibility of an intermediate frequency range wherein the tanh function saturates but $|\lambda/K|$ is still negligible. Under these

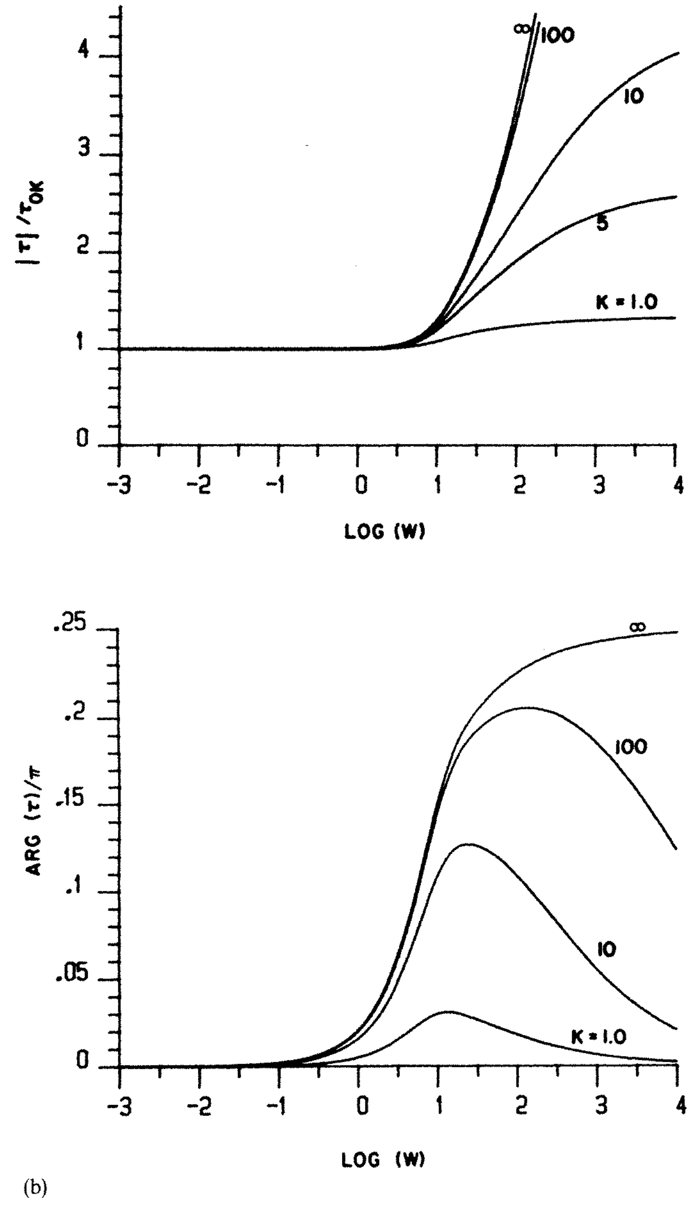

Figure 3. Magnitude (a) and phase (b) of τ relative to the low-frequency limit $\tau_{0K} = \tau_0/(1 + 3/K)$, for constant viscosity

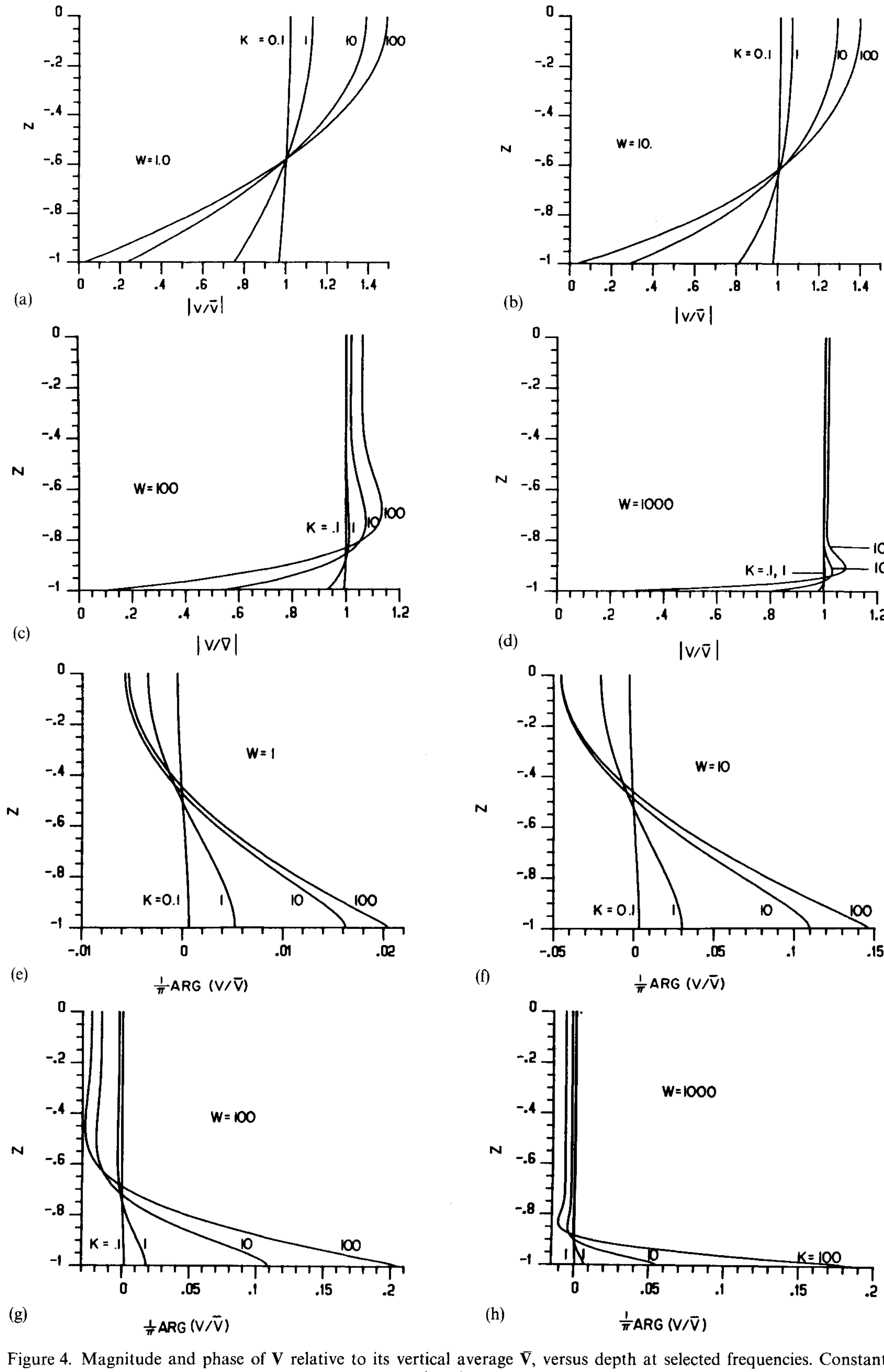

Figure 4. Magnitude and phase of **V** relative to its vertical average $\bar{\mathbf{V}}$, versus depth at selected frequencies. Constant viscosity

conditions, τ approaches the asymptote

$$\tau = \frac{\tau_0 \lambda}{3} = \frac{\tau_0}{3}\sqrt{(jW)}, \tag{37}$$

with the argument of τ approaching 45°. For very large K, this intermediate range can be significant, and extends to arbitrarily high frequencies for the no-slip case.

In Figures 2 and 3 we plot versus frequency the amplitude and phase of $\bar{\mathbf{V}}$ relative to $\mathbf{V}_0$, and of τ relative to $\tau_0/(1 + 3/K)$, for various values of K. The intermediate frequency range wherein $\arg(\tau)$ tends toward 45° is apparent. Additionally, Figure 4 shows versus depth the amplitude and phase of $\mathbf{V}$ relative to $\bar{\mathbf{V}}$. The phase shift through the depth can be seen to approach 45° in the mid-frequency, high K range, e.g. $W = 100$, $K = 100$*. In this particular case the 'intermediate' nature of the solution is clearly visible: a vertically uniform top layer roughly 1/2 the total depth, underlain by a shear layer where bottom stress is sufficient to hold the velocity near zero at the bottom. At $W = 100$, the total depth is roughly 7 times the skin depth.

Finally, the vertically averaged force balance is illustrated in Figure 5 as a set of complex plane plots of the gravity, inertia and friction phasors. The transition from low- to high-frequency asymptotes is evident.

To put the dimensionless groups in perspective, consider the diurnal tide (period = 12·4 h) in a shallow sea, 20 m deep. With typical values of $N = 0{\cdot}0025\ \mathrm{m^2/s}$ and $k = 0{\cdot}002\ \mathrm{m/s}$, we find $W = 22$, $K = 16$, which is clearly in the transition range. With $H = 100$ m, we have $W = 560$, $K = 80$, again in the range where $\mathrm{Im}(\tau)$ is significant.

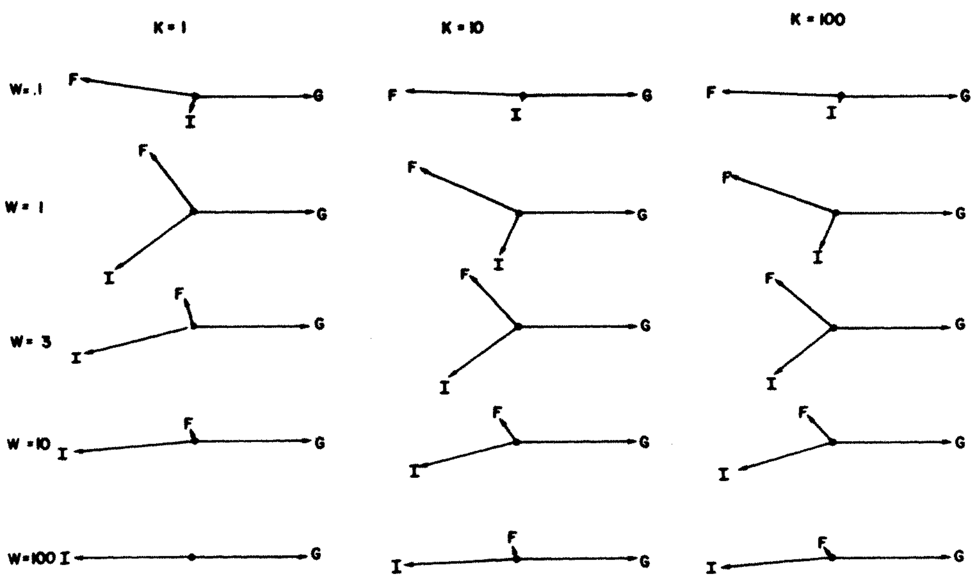

Figure 5. Complex plane phasor balance among gravity (G), inertia (I), and friction (F) forces at various combinations of W and K. Constant viscosity

*Physically, the phase lead of bottom currents in oscillatory flow is well established. See Reference 13, for instance.

VERTICAL STRUCTURE AND BOTTOM STRESS WITH ROTATION

At this point it is convenient to introduce the complex scalar velocity components (u, v) and to explicitly write out the scalar components of the momentum equation (2), which are coupled by the Coriolis terms:

$$j\omega u - fv - \frac{\partial}{\partial z}\left(N\frac{\partial u}{\partial z}\right) = -g\frac{\partial \zeta}{\partial x}, \tag{38}$$

$$j\omega v + fu - \frac{\partial}{\partial z}\left(N\frac{\partial v}{\partial z}\right) = -g\frac{\partial \zeta}{\partial y}, \tag{39}$$

with boundary conditions (3), (4) as before. These may be uncoupled by introduction of two linear combinations of u and v:

$$v^+ = \frac{u + jv}{2}, \tag{40}$$

$$v^- = \frac{u - jv}{2}. \tag{41}$$

The same linear combinations of (38), (39) then give

$$v^+ - \frac{\partial}{\partial Z}\left(\frac{N}{j(\omega + f)H^2}\frac{\partial v^+}{\partial Z}\right) = v_0^+, \tag{42}$$

$$v^- - \frac{\partial}{\partial Z}\left(\frac{N}{j(\omega - f)H^2}\frac{\partial v^-}{\partial Z}\right) = v_0^-, \tag{43}$$

with gravity terms

$$v_0^+ = \frac{1}{2}\left(-g\frac{\partial \zeta}{\partial x} - jg\frac{\partial \zeta}{\partial y}\right)\Big/ j(\omega + f), \tag{44}$$

$$v_0^- = \frac{1}{2}\left(-g\frac{\partial \zeta}{\partial x} + jg\frac{\partial \zeta}{\partial y}\right)\Big/ j(\omega - f). \tag{45}$$

Boundary conditions are

$$\frac{\partial v^+}{\partial Z} = \frac{kH}{N}v^+, \quad \text{at } Z = -1, \tag{46}$$

$$= 0 \qquad , \text{at } Z = 0, \tag{47}$$

and similarly for v^-. The equations for v^+ and v^- are completely uncoupled and identical to (8), (9) with the important introduction of $\omega \pm f$ in place of ω. Solutions are thus

$$v^+ = v_0^+\left[1 - \frac{A^+}{B^+}\right], \tag{48}$$

$$\bar{v}^+ = v_0^+\left[1 - \frac{\overline{A^+}}{B^+}\right], \tag{49}$$

and similarly for v^-. Also, we obtain two different bottom stress coefficients, based on the shifted frequencies $\omega \pm f$:

$$\tau^{+} = \frac{j(\omega + f)\overline{A^{+}}}{B^{+} - \overline{A^{+}}}, \qquad \tau^{-} = \frac{j(\omega - f)\overline{A^{-}}}{B^{-} - \overline{A^{-}}} \tag{50}$$

The scalar velocity components are then obtained by inverting (40), (41):

$$u = v^{+} + v^{-}, \tag{51}$$

$$v = \frac{1}{j}(v^{+} - v^{-}). \tag{52}$$

Successful decoupling of the horizontal and vertical structures requires expression of the bottom stress in terms of $\bar{u}, \bar{v}$. The x-component of bottom stress is

$$N\frac{\partial u}{\partial z}\bigg|_{-H} = ku|_{-H} = k(v^{+} + v^{-})|_{-H} = H(\tau^{+}\overline{v^{+}} + \tau^{-}\overline{v^{-}}), \tag{53}$$

and use of (40), (41) yields the desired result

$$N\frac{\partial u}{\partial z}\bigg|_{-H} = H\left(\frac{\tau^{+} + \tau^{-}}{2}\right)\bar{u} + jH\left(\frac{\tau^{+} - \tau^{-}}{2}\right)\bar{v}. \tag{54}$$

The same procedure yields for the y-component of bottom stress

$$N\frac{\partial v}{\partial z}\bigg|_{-H} = H\left(\frac{\tau^{+} + \tau^{-}}{2}\right)\bar{v} - jH\left(\frac{\tau^{+} - \tau^{-}}{2}\right)\bar{u}. \tag{55}$$

Incorporation of (54), (55) into the vertically averaged form of (38), (39) yields equations in $(\zeta, \bar{u}, \bar{v})$ only:

$$j\omega\bar{u} - f'\bar{v} + \tau'\bar{u} = -g\frac{\partial \zeta}{\partial x}, \tag{56}$$

$$j\omega\bar{v} + f'\bar{u} + \tau'\bar{v} = -g\frac{\partial \zeta}{\partial y}, \tag{57}$$

with

$$\tau' = \frac{\tau^{+} + \tau^{-}}{2}, \tag{58}$$

$$f' = f - j\left(\frac{\tau^{+} - \tau^{-}}{2}\right). \tag{59}$$

Note that the bottom stress creates a complex, Coriolis-like term in the vertically averaged equations, manifest in the apparent shift from f to f'. Remarkably, though, all of the vertical structure is embodied in the complex coefficients τ' and f', such that solutions for ζ may still be obtained from (7) alone. With ζ in hand, v^{+} and v^{-} may then be obtained as in (48) and, finally, u and v obtained from (51), (52). As in the rotation-free case, the essential new relationships are those relating τ^{+} and τ^{-} to the physical parameters of the problem, equations (20)–(22).

We may estimate the magnitude of f' by noting that $\tau^{+} - \tau^{-}$ is the change in τ over the frequency interval $\Delta\omega = 2f$. Thus,

$$f' \simeq f\left[1 - j\frac{\partial \tau}{\partial \omega}\right]. \tag{60}$$

For the constant viscosity, intermediate frequency case we have the simple asymptote (37) for τ, and differentiation yields

$$f' \simeq f\left[1 + \frac{1}{2\sqrt{(jW)}}\right]. \tag{61}$$

It appears that the bottom stress contribution to f' is in magnitude roughly 10 per cent or less, for this particular case.

As a concrete example, consider the diurnal tide in a 20 m sea at mid-latitude. With $\omega = 1{\cdot}4 \times 10^{-4}\,\mathrm{s}^{-1}$; $f = 10^{-4}\,\mathrm{s}^{-1}$; $H = 20\,\mathrm{m}$; $N = 0{\cdot}0025\,\mathrm{m}^2/\mathrm{s}$ and $k = 0{\cdot}002\,\mathrm{m/s}$, we find

$$\tau^+ = (2{\cdot}835, 1{\cdot}414) \times 10^{-5},$$
$$\tau^- = (1{\cdot}707, 0{\cdot}5262) \times 10^{-5}.$$

and

$$\frac{\tau^+ - \tau^-}{2} = (0{\cdot}564, 0{\cdot}426) \times 10^{-5},$$

which in magnitude is 7 per cent of f.

Finally, the v^+, v^- have a direct, intuitive interpretation. Let $(\mathscr{u}, \mathscr{v})$ be the actual time-dependent components of velocity:

$$\mathscr{u} = \mathrm{Re}(u e^{j\omega t}), \tag{62}$$

$$\mathscr{v} = \mathrm{Re}(v e^{j\omega t}). \tag{63}$$

The complex velocity $\mathscr{u} + j\mathscr{v}$ may be expressed as the sum of clockwise and counterclockwise rotating vectors in the complex plane:[12]

$$\mathscr{u} + j\mathscr{v} = v^+ e^{j\omega t} + v^{-*} e^{-j\omega t}, \tag{64}$$

where the asterisk indicates the complex conjugate. If we let $\phi^+ \equiv \arg(v^+)$, and $\phi^- \equiv \arg(v^-)$, then

$$\mathscr{u} + j\mathscr{v} = |v^+| e^{j(\omega t + \phi^+)} + |v^-| e^{-j(\omega t + \phi^-)} \tag{65}$$

and the current ellipse at any depth is characterized as in Reference 12 by the following parameters:

maximum speed: $|v^+| + |v^-|$
minimum speed: $||v^+| - |v^-||$

time of max. speed: $-\dfrac{(\phi^+ + \phi^-)}{2\omega}$

angle between major axis and x-axis: $\dfrac{\phi^+ - \phi^-}{2}$

sense of rotation: counterclockwise iff $|v^+| > |v^-|$.

CONCLUSIONS

The principal objective of this paper is to provide exact solutions for three-dimensional hydrodynamic model testing. Such solutions may be assembled from conventional solutions to (a) the two-dimensional vertically averaged equations, and (b) the 1-D vertical diffusion equation. The key linkage is the expression of bottom stress in terms of $\bar{\mathbf{V}}$. This expression, which is not part of the original 3-D problem formulation, is derived herein for arbitrary $N(z)$ in terms of the homogeneous solutions of the diffusion equation.

The bottom stress coefficient τ depends upon frequency and is generally complex, indicating a phase difference between bottom stress and $\bar{\mathbf{V}}$. For the special case $\partial N/\partial z = 0$ this phase lead can be as high as 45°, and this occurs in the intermediate frequency range where the depth is divided roughly equally between an upper homogeneous zone and a lower boundary layer.

When rotation is present the bottom stress contributes a complex Coriolis-like term to the vertically averaged equations. The magnitude of this term is roughly 10 per cent or less of the Coriolis acceleration and depends upon frequency; it is most pronounced in the intermediate frequency range.

ACKNOWLEDGEMENTS

This work was supported by the U.S. Office of Naval Research, contracts N00014-81K-0550 and 83K-0359; and by the U.S. National Science Foundation, grant #CEE 83-52226.

REFERENCES

1. A. M. Davies, 'Formulation of a three-dimensional hydrodynamic sea model using a Galerkin-eigenfunction method', *Int. J. Num. Meth. Fluids*, **3**, 33–60 (1983).
2. D. R. Lynch and W. G. Gray, 'Analytic solutions for computer flow model testing', *J. Hydraul. Div. ASCE*, **104**, (HY10), 1409–1428 (1978).
3. M. Rahman, 'Analytical solutions for tidal propagation in a rectangular basin', *Advances in Water Resources*, **6**, 44–53 (1983).
4. D. Prandle and M. Rahman, 'Tidal response in estuaries', *J. Phys. Oceanogr.*, **10**, 1552–1573 (1980).
5. D-P. Wang, 'Wing-driven circulation in the Chesapeake Bay, winter 1975', *J. Phys. Oceanogr.*, **9**, 564–572 (1979).
6. J. H. Thomas, 'A theory of steady wind-driven currents in shallow water with variable eddy viscosity', *J. Phys. Oceanogr.*, **5**, 136–142 (1975).
7. A. J. Witten and J. H. Thomas, 'Steady wind-driven currents in a large lake with depth-dependent eddy viscosity', *J. Phys. Oceanogr.*, **6**, 85–92 (1976).
8. P. Welander, 'Wind action on a shallow sea: some generalizations of Ekman's theory', *Tellus*, **9**, 45–52 (1957).
9. G. Z. Forristall, 'Three-dimensional structure of storm-generated currents', *J. Geophys. Res.*, **79**, (18), 2721–2729 (1974).
10. O. S. Madsen, 'A realistic model of the wind-induced Ekman boundary layer', *J. Phys. Oceanogr.*, **7**, 248–255 (1977).
11. T. F. Jordan and J. R. Baker, 'Vertical structure of time-dependent flow dominated by friction in a well-mixed fluid', *J. Phys. Oceanogr.*, **10**, 1091–1103 (1980).
12. D. Prandle, 'The vertical structure of tidal currents', *Geophys. Astrophys. Fluid Dynamics*, **22**, 29–49 (1982).
13. P. K. Kundu, J. O. Blanton and M. M. Janopaul, 'Analysis of current observations on the Georgia shelf', *J. Phys. Oceanogr.*, **11**, (8), 1139–1149 (1981).